A STUDY OF MUSCLE CONTROL WITH TWO FEEDBACK CONTROLS FOR POSTURE AND REACTION FORCE FOR MORE ACCURATE PREDICTION OF OCCUPANT KINEMATICS IN LOW-SPEED FRONTAL IMPACTS

Daichi Kato
Yuko Nakahira
Masami Iwamoto
Toyota Central R&D Labs., Inc.
Japan

Paper Number 17-0004

ABSTRACT

In future automotive crashes that involve advanced safety vehicles or autonomous vehicles, the number of minor or moderate injuries may increase because of vehicle slowing by safety systems such as autonomous emergency brakes. Recent studies suggest that pre-crash muscle activity of occupants could have significant effects on the kinematics of occupants in such situations. In previous studies, we developed a human body finite element (FE) model with whole-body muscles and a muscle controller with posture control to predict relaxed occupant kinematics during deceleration. However, the controller could not predict tensed-occupant kinematics. The objective of this study is to develop a muscle controller for more accurate prediction of relaxed- and tensed-occupant kinematics and to validate it in low-speed frontal crash situations.

Total HUman Model for Safety (THUMS) version 5, including 262 one-dimensional Hill-type muscle models, is used and a new muscle controller using proportional-integral-derivative (PID) control is developed. The controller has two feedback controls involving three-dimensional angles of 16 joints and reaction forces using a steering wheel and pedals. The control of each joint angle works to return to the initial joint angle in order to maintain overall body posture. The control of each reaction force works to achieve a pre-determined target force. The controller is validated using a series of experimental data from cadaver and volunteer tests reproducing low-speed frontal impacts with peak sled accelerations of 2.5 G and 5.0 G, which are obtained from the literature.

Simulation results demonstrate that head excursions predicted without any control and when using only posture control are similar to excursions from cadaver and relaxed volunteer test data, respectively. Head excursions predicted by a total controller with the two feedback controls of posture and force show a tendency similar to that for tensed volunteers. The forces predicted by the total controller are similar to those for the tensed volunteer test data for the pedals but not for the steering wheel.

Further studies on optimization methods are needed in order to determine valid PID gain parameters in various dynamic environments. THUMS using the developed controller shows the potential for representation of both relaxed- and tensed-occupant kinematics during low-speed impact decelerations.

INTRODUCTION

Recently, active safety systems such as autonomous emergency brakes (AEB) have been developed and implemented by several automobile manufacturers in cars on the market to prevent imminent accidents and thereby to reduce the number of fatalities more effectively than with only passive safety systems. In future automotive crashes involving advanced safety vehicles or autonomous vehicles, the number of severe injuries may decrease because of reduced vehicular impact speeds owing to pre-crash technology such as AEBs. However, we consider that the number of minor or moderate injuries with different tendencies from those of high-speed frontal collisions may increase due to possible changes in occupant kinematics owing to AEBs.

Ejima et al. [1] performed a series of volunteer tests using adult male subjects seated on a frontal impact sled system with a peak deceleration of 0.8 G, corresponding to that of a pre-crash event, with AEBs. They found that occupant kinematics with relaxed muscle conditions, i.e., assuming that the occupant does not anticipate a collision, were different from those for the tensed-muscle condition, i.e., in which the occupant anticipates a collision, and that occupant muscle activity could change postures just before collisions. Beeman et al. [2,3] performed a series of experimental tests with five male volunteers and three cadavers using a frontal sled with peak accelerations of 2.5 and 5.0 G, which simulated low-speed crash decelerations. They found that muscle activity could have significant effects on occupant kinematics during low-speed frontal impacts.

Some researchers have developed computational human models with active muscles. Human models are useful for investigating muscle activity effects on occupant behavior both in pre-crash and during crash events; in contrast, it is very difficult in volunteer tests to reproduce various crash situations. Meijer et al. [4] developed a multi-body human model including the muscles of the neck, arms, and legs. Each human body part was modeled as a rigid body, each joint was modeled with a mechanical joint, and each muscle was modeled using Hill-type muscle elements. They applied their model to prediction of occupant behavior during braking and impact by using proportional-integral-derivative (PID) control and tried to represent relaxed and braced muscle conditions by setting co-contraction levels of antagonist muscles. Östh et al. [5] developed a human body finite element (FE) model with some muscles in the neck, trunk, and upper extremities. They incorporated muscles modeled using Hill-type muscle elements into a human body FE model called Total HUman Model for Safety (THUMS) version 3 [6], and applied their model to predicting occupant behaviors during decelerations applied by AEB or driver braking. Furthermore, they attempted to represent occupants with different muscle activity conditions by changing the reference posture control positions [7].

These researchers estimated occupant muscle activations using posture control with PID control by using information about translational and rotational displacements of joints or feature points. However, especially in braced conditions, some forces at contact areas between the human body and the vehicle interior may affect occupant behavior in pre-crash and during a crash. Hault-Dubrulle et al. [8] conducted a series of volunteer tests to analyze the behavior of 80 drivers during critical events using a driving simulator. They showed that forces exerted on the steering wheel and the brake pedal during collisions increased on average by approximately 37% and 51%, respectively, in comparison with normal driving. Beeman et al. [2] showed that elbow and knee joint angles were extended with increased forces at the steering wheel or pedals in the braced condition in comparison with the relaxed condition. Therefore, forces generated by muscles are important in predicting occupant behavior in the braced condition.

The objective of this study is to develop a new muscle controller with two feedback controls for posture and reaction forces imparted at the steering wheel and pedals for more accurate prediction of occupant kinematics with various muscle activations. We apply the developed controller to a human body model and validate it against volunteer test data obtained in dynamic circumstances of low-speed frontal crash situations. In addition, a braced condition reproduced by using constant muscle activation levels based on electromyography (EMG) data as in the previous study [9] is compared with the braced condition reproduced by the developed controller.

METHODS

In this study, we developed a muscle activation controller for whole-body muscles for THUMS version 5 to estimate occupant muscle activations by posture control with PID control [10]. THUMS is a computational human body FE model with a

total number of around 280,000 elements and has anatomical structures including the bones, skin, internal organs, brain, ligaments, and muscles. The muscle parts of THUMS were modeled with Hill-type muscle properties, and each muscle had the capability of generating forces according to activation levels given by the activation controller at each time step. Muscle activation control was performed in parallel with FE simulation. In our previous study, the muscle controller was developed using Linux C++ and estimated whole-body occupant kinematics during low-speed impact deceleration using THUMS version 5 and MPP LS-DYNA version 971 R6.1.2 single-precision (LSTC, USA). However, MPP LS-DYNA R8.0.0 single-precision (LSTC, USA) was released in 2015, and a PID controller was newly added as an internal function. By using this function, we have recently developed a controller for head-neck muscles for posture control so that simulations with muscle controls can be performed using only LS-DYNA [11]. In this study, we expanded the head-neck muscle controller to whole-body muscles. In addition, the calculation methods for each joint angle and for the muscle controller were modified.

We newly developed a muscle controller for reaction force control using PID control and integrated it with the posture control to represent braced conditions of volunteers as shown in Figure 1. The following section describes the definition of joints and the calculation method for each joint angle as well as the muscle controller for posture control, reaction force control, and total control of posture and force.

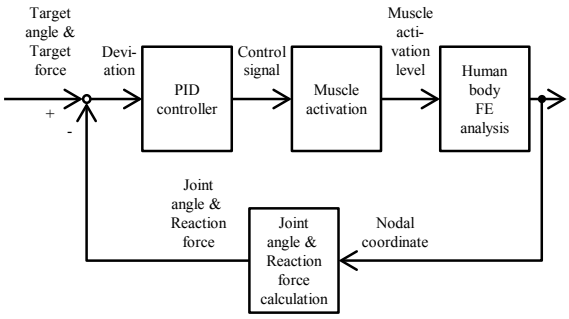

Figure 1. The developed muscle activation controller.

Definition of Joints and Calculation Method for Joint Angles in the New Muscle Controller

In an update of previous studies [10,11], the human whole-body was divided into 17 body parts, where the trunk was divided coarsely into the thorax and the pelvis for simplification, as shown in Figure 2. In addition, the new muscle controller covered a total of 36 rotations in the anatomical joints between body parts as follows:

• Assumed neck joint: lateral flexion (1), flexion-extension (2), left rotation-right rotation (3),

• Assumed trunk joint: lateral flexion (4), flexion-extension (5), left rotation-right rotation (6),

• Hip joints: adduction-abduction (7, 8), extension-flexion (9, 10), internal rotation-external rotation (11, 12),

• Knee joints: flexion-extension (13, 14),

• Ankle joints: inversion-eversion (15, 16), plantar flexion-dorsiflexion (17, 18),

• Assumed scapulo-thoracic (ST) joints: depression-elevation (19, 20), flexion-extension (21, 22),

• Shoulder joints: adduction-abduction (23, 24), backward extension-forward flexion (25, 26), internal rotation-external rotation (27, 28),

• Elbow joints: extension-flexion (29, 30), pronation-supination (31, 32),

• Wrist joints: ulnar deviation-radial deviation (33, 34), extension-flexion (35, 36).

The posture of the scapulas and the upper arms were defined based on the thorax posture in definitions of the ST and shoulder joints.

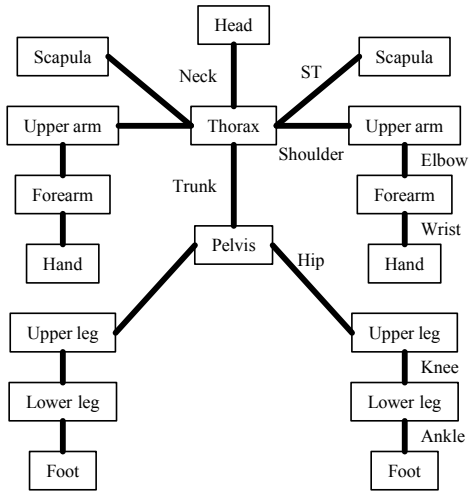

Figure 2. Definition of body parts and joints.

A main point of modification from the previous muscle controller for posture control is the

calculation method for joint angles. In previous studies [5,10], each joint angle of the FE model, in which joints were not defined by mechanical joints, was calculated as an angle between three points. However, when considering three-dimensional angles for each joint, the previous method cannot express rotation around an axis linking two points. Therefore, in this study, we introduced a new method for calculating joint angles in the FE model. Each joint angle is calculated by the following procedure:

1. Select three nodes in each body part among the 17 body parts to define a local coordinate system in the body part.

2. Define a base vector set of the local coordinate system in each body part. For example, as shown in Figure 3, when the selected X-Y plane is defined by three nodes and two vectors of X1 and Y1 out of the three nodes, including the origin, are defined, the X axis is set along the vector X1 and the Z axis is obtained from the cross product of X1 and Y1. In addition, when a vector Z1 is defined along the Z axis, the Y axis is obtained from a cross product of Z1 and X1. The base vector set for a body part is defined along the three axes as three vectors whose sizes are 1.

3. Calculate the rotation matrix of each joint from two base vector sets of two adjacent body parts. For example, the base vector sets of the thorax and the head coordinate systems are used to calculate the neck joint angle.

4. Convert the rotation matrix into Cartesian rotation vectors in the direction of the rotation axis and with lengths equal to the amplitude of the rotation [12].

5. Express the Cartesian rotation vectors in a local coordinate system on the side close to the pelvis among the two local coordinate systems. For example, in the neck joint, the Cartesian rotation vector is expressed in the thorax coordinate system.

Cartesian rotation vectors are more advantageous compared with other expressions of rotation angles such as Euler angles from the viewpoints of easy geometrical interpretation and the absence of kinematic singularities.

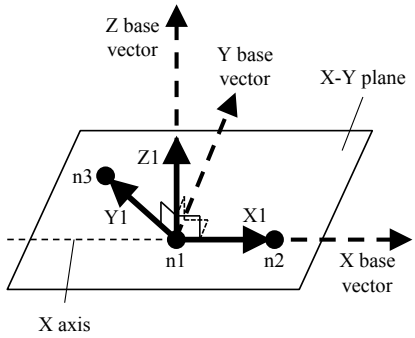

Figure 3. Definition of a local coordinate system.

Development of a Muscle Controller for Posture Control

The posture control was modified somewhat from that reported in the previous study [10]. The PID controllers were represented by the PIDCTL function implemented in LS-DYNA. The controller function calculates control signals u_j based on the errors e_j (rad), which are differences between each joint angle and each target angle defined as follows:

$$u_j(t_n) = k_{\mathrm{P}j} \cdot e_j(t_n) + k_{\mathrm{I}j} \cdot \int_0^{t_n} e_j(\tau)\mathrm{d}\tau + k_{\mathrm{D}j} \cdot \frac{\mathrm{d}e_j(t_n)}{\mathrm{dt}}$$

(Equation 1)

where the subscript index j (=1, …, 36) represents each of the 36 rotations covered by the controller, $k_{\mathrm{P}j}$ (rad^{-1}), $k_{\mathrm{I}j}$ (rad^{-1} s^{-1}), and $k_{\mathrm{D}j}$ (s/rad) are PID gains, and t_n (s) is the current time step. Furthermore, the target angle was set as the initial joint angle to maintain the initial posture of the model.

The calculation of muscle activation levels was based on the expression [10] describing the firing rate of muscle motor neurons using a sigmoid curve. Muscle activation levels $a_{\mathrm{posture}\,i}$ with a range of 0 to 1 were calculated according to

$$a_{\mathrm{posture}\,i}(t_n) = A_i^0 + C_i \cdot s_i,$$

$$s_i = \frac{1}{1+\exp\left(-S \cdot w_i + B\right)}, w_i = \sum_j R_{ij} \cdot u_i(t_n)$$

(Equation 2)

where the subscript index i (=1, …, 218) represents each of the 218 muscles except for muscles of the hands and the feet, A_i^0 are base activation levels, C_i are muscle activation coefficients, S and B are constants of a sigmoid curve, s_i are sigmoid curves, and w_i are intermediate variables. In addition, R_{ij} are the percentage contributions of each muscle to each joint motion, which were determined according to the information on the role of each muscle described in anatomical texts (e.g. [13]). For example, we show some percentage contributions R_{ij} of right lower-extremity muscles for hip and knee joint motions in Table A1. This expression formula using a sigmoid curve is one of the hypotheses used in this study, but it has the potential to express the threshold of muscle firing using the constants S and B. However, because of a lack of data for expressing the threshold quantitatively, in this study, the constants S and B were provisionally set to 9.19 and 4.60 respectively; these values were adjusted so that the sigmoid curve changed from 0.01 to 0.99 while the intermediate variables w_i changed from 0 to 1.

Development of a Muscle Controller for Reaction Force Control

In the muscle controller for reaction forces, first the error between each estimated reaction force and each target force was obtained. The estimated reaction force was calculated as described in the Appendices. The target forces were set to 300 N for each hand and 400 N for each foot in this study based on forces measured from a volunteer test on a braced occupant [3]. Next, control signals v_h were calculated based on the errors ε_h (N) as follows:

$$v_h(t_n) = K_{\mathrm{P}h} \cdot \varepsilon_h(t_n) + K_{\mathrm{I}h} \cdot \int_0^{t_n} \varepsilon_h(\tau)\mathrm{d}\tau + K_{\mathrm{D}h} \cdot \frac{\mathrm{d}\varepsilon_h(t_n)}{\mathrm{dt}}$$

(Equation 3)

where the subscript index h (=1, …, 4) represents each force exerted by the hand or foot on the right or left side and $K_{\mathrm{P}h}$ (N^{-1}), $K_{\mathrm{I}h}$ ($\mathrm{N}^{-1}\ \mathrm{s}^{-1}$), and $K_{\mathrm{D}h}$ (s/N) are PID gains. Finally, muscle activation levels $a_{\mathrm{force}\,i}$ for force control were calculated according to

$$a_{\mathrm{force}\,i}(t_n) = \sum_h P_{ih} \cdot v_h(t_n)$$

(Equation 4)

where P_{ih} are the percentage contributions of each muscle to the pushing force. The values of P_{ih} were determined according to anatomical texts (e.g. [13]) wherein the role of each muscle is described, and the measured EMG data were obtained from volunteer tests in a braced situation [14]. Specifically, we set values in the range from 0 to 0.3 for P_{ih} so that the ST and shoulder joints had flexion, the elbow joints had extension, the wrist joints had ulnar deviation and flexion, the hip joints had extension, the knee joints had extension, the ankle joints had plantar flexion, and the trunk had extension. For example, we also show some percentage contributions P_{ih} of the right lower-extremity muscles to pushing forces on the right pedal in Table A1.

In the total control of posture and force for reproducing braced conditions, muscle activation levels $a_{\mathrm{total}\,i}$ were calculated according to

$$a_{\mathrm{total}\,i}(t_n) = a_{\mathrm{posture}\,i}(t_n) + a_{\mathrm{force}\,i}(t_n).$$

(Equation 5)

Validation of Frontal Impact Responses

The posture control and the total controller were applied to THUMS version 5, which has a body size in the 50th percentile of the American adult male (AM50) population with a sitting posture, and validated against a series of volunteer and cadaver test data obtained from the literature [3].

Beeman et al. [3] conducted a series of frontal sled tests using five male volunteers of approximately AM50 body size and three male cadavers. The peak decelerations of the sled were 2.5 G and 5.0 G for these groups, which are equivalent to collisions at 4.8 km/h and 9.7 km/h, respectively. Each volunteer was exposed to two sled impulses under two muscle conditions, i.e., relaxed and braced states. All subjects of the tests sat on a rigid seat equipped with a three-point seatbelt and

placed their feet on the foot plates and their hands on the simulated steering wheel. Occupant motions during decelerations were measured using a three-dimensional motion-capturing system.

Simulation setups were reproduced using THUMS similar to the abovementioned experimental setups, as shown in Figure 4. In particular, the initial posture of the human subject in each test condition was reproduced carefully. We validated our muscle controller by comparing excursions of the head's center of gravity (CG) because head excursion is critical to understanding occupant kinematics in frontal crashes. We performed the simulations without muscle activation to reproduce cadaveric conditions, with posture control to reproduce the relaxed volunteer conditions, and with total control of posture and force to reproduce the braced or tensed-volunteer conditions.

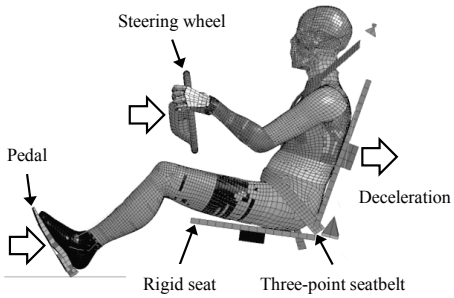

Figure 4. Simulation setup for representing frontal sled tests [3].

RESULTS

Tuning of Control Parameters

In order to apply the muscle controller to the human body model, tuning of control parameters is required. In this study, parameters for posture control were first determined by trial and error based on comparison with experimental data in relaxed volunteer conditions. For simplification, common controller gains for posture control were used in each of the three parts of the trunk and neck, upper extremity, and lower extremity, and their P gains were set to 8 rad^{-1}, 10 rad^{-1}, and 2 rad^{-1}, respectively. On the other hand, the I and D gains for posture control were set to zero values based on parametric studies which we performed to investigate the effects of I and D gains on occupant behavior. Next, using the determined posture control gains, parameters for force control were determined by trial and error based on comparison with experimental data in tensed volunteer conditions. Common controller gains were used for all contact parts, and the P, I, and D gains were set to 0.002 N^{-1}, 0.1 N^{-1} s^{-1}, and 0 s/N, respectively.

Comparison of Head CG Excursions

Figure 5 shows head CG excursions in the forward and downward directions during decelerations. Simulation results were compared with test data obtained from Beeman et al. [3]. In each deceleration of 5.0 G and 2.5 G, cadaver test data, volunteer test data in relaxed conditions, and those with braced conditions were compared with simulation results with no control, posture control, and total control of posture and force, respectively. In addition, simulation results in the braced condition reproduced by using constant muscle activation levels based on EMG data as used in the previous study [9] were also compared for the volunteer test data in braced conditions. The EMG data are indicated as "EMG-based muscle activation" hereafter, and are shown by dotted lines.

Figure 5 shows that the head excursions of cadavers tended to be larger than those of volunteers, and the simulation results had similar tendencies in both decelerations. In addition, simulation results were generally within the range of dispersion of cadaver tests. The excursions of relaxed volunteers tended to be smaller in downward displacements than those of cadavers and braced volunteers. The excursions of braced volunteers tended to have linear downward displacements in the initial period (Figures 5(e) and 5(f)). The downward displacements of simulation results with total control of posture and force were almost the same as for the test data while those with EMG-based muscle activation could not constrain head excursions sufficiently. As shown in Figure 5, simulation results using the developed muscle controller showed general agreement with test data regarding head CG excursions.

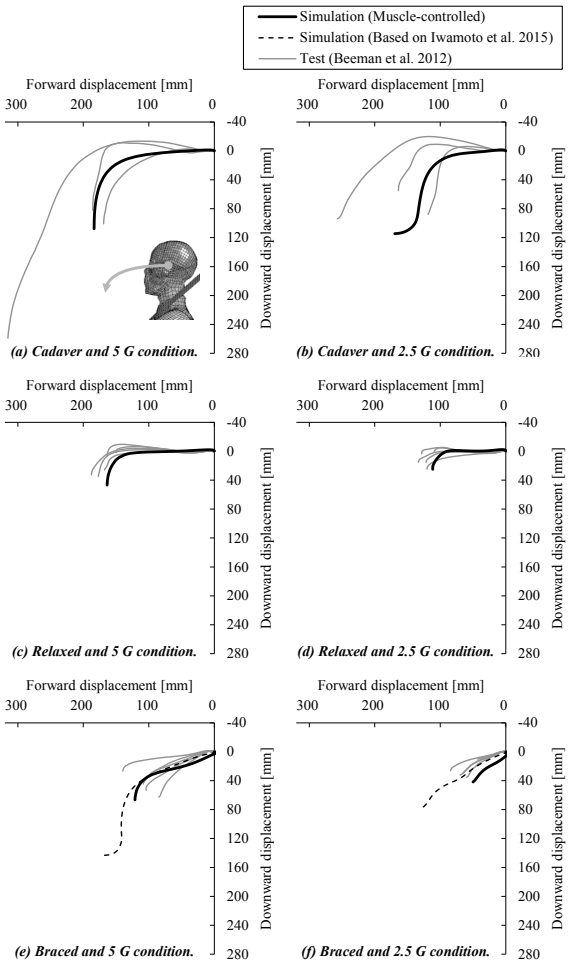

Figure 5. Comparisons of head CG excursions in impact conditions of 5.0 G and 2.5 G decelerations.

Comparison of the Reaction Forces

Figure 6 shows the resultant reaction forces from the steering wheel or right pedal in the braced condition. Figure 6 also shows the simulation results for a braced condition with EMG-based muscle activation. Simulation results with total control of posture and force were compared with the average values of test results measured by Beeman et al. [3]. The time 0 s is defined as the time when the input of deceleration was started. In the simulations, the braced conditions were reproduced 0.2 seconds before the input.

Figures 6(a) and 6(b) show the steering wheel forces. Since the force was measured at the steering column in the experiment, we compared the predicted resultant force, which summed the forces of the left and right hands, with those from volunteer test data. The tendency of changes in the time histories of the predicted forces was similar to those of the test data, but the magnitude of the predicted force was smaller than that of the test data in each deceleration. However, the simulation results with muscle activations predicted by the developed controller showed larger forces than those with EMG-based muscle activation.

Figures 6(c) and 6(d) show the right pedal forces. The forces in the simulation results at the time of 0 s were approximately equal to those of the test data in both decelerations. The forces of the left pedal were approximately equal to those of the right pedal.

In addition, the CORrelation and Analysis (CORA) method proposed by Gehre et al. [15,16] was used for a quantitative evaluation of simulation results. CORA release 3.6 was used, and the parameter setting was similar to the previonus study [9]. This method was available only for time history data, and evaluates the overall degree of coincidence objectively between the simulation results and experimental data. The sliding scale of CORA is defined in technical report ISO/TR 9790, and evaluated with five phases of “Excellent”, “Good”, “Fair”, “Marginal”, and “Unacceptable”. Table 1 shows the CORA evaluations for simulation results with muscle control. The CORA evaluations for the steering column force and the right pedal force were “Fair” and “Good”, respectively.

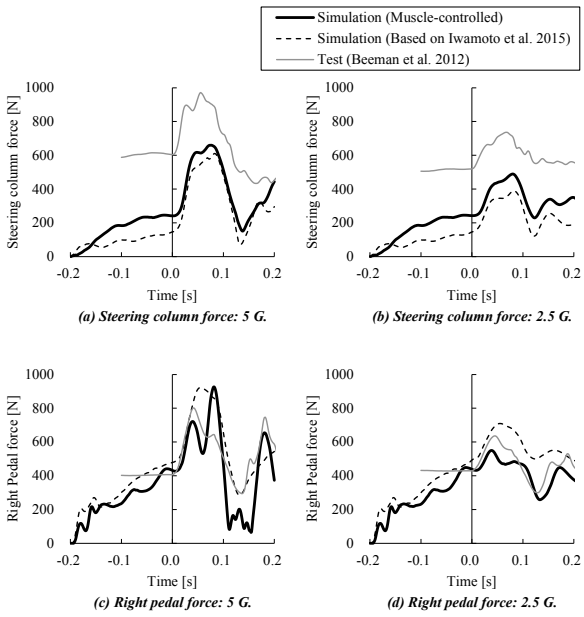

Figure 6. Comparisons of reaction forces in the braced condition.

Table 1.
The CORA evaluations for reaction forces in the braced condition with muscle control.

Force	Deceler-ation	Corridor method rating	Correlation Method			Correl-ation method rating	Total rating	Evalu-ation
			Cross correl-ation	Size	Phase shift			
Steeing column	5G	0.293	0.888	0.388	1.000	0.791	0.542	Fair
	2G	0.196	0.948	0.332	1.000	0.807	0.502	Fair
Right pedal	5G	0.544	0.744	0.876	1.000	0.841	0.693	Good
	2G	0.733	0.957	0.746	1.000	0.915	0.824	Good

DISCUSSION

Determining Control Parameters

Östh et al. [5] determined the gains of their PID controller for prediction of muscle activation using a radial basis function meta-model sampled by performing 144 simulations. Furthermore, the initial value for their optimization was based on iterative calculation used in their previous study. On the other hand, Rooij [17] used different control parameters for each simulation condition. The parameters were originally found by optimization [18]; however, the parameters were changed using estimates for each test condition. Thus, a large number of calculations and significant experience are required to determine control parameters.

Since the whole-body FE model that we used is not suitable for optimization calculations used to determine the control parameters owing to a problem of computational costs, in this study, we reduced the number of gain parameters for simplification, and determined their values by trial and error.

The determination of PID gains is one of the primary problems for researchers using PID controllers for muscle control. Further study of optimization methods is needed in order to determine valid gain parameters for predicting occupant behavior in various dynamic environments.

Effects of the Muscle Controller

In this study, we attempted to reproduce the cases of volunteers for two muscle conditions of relaxed and braced states during low-speed frontal impacts using THUMS version 5 and a newly developed muscle controller.

Comparisons between simulation results for cadaver test data and for relaxed volunteer test data as shown in Figure 5 indicate that the posture controller has the potential to reduce downward displacement of the head. Since the posture controller decreased the flexions of the neck and trunk, the head excursions decreased and showed a similar tendency for the relaxed volunteer test data. From comparisons between simulation results for the relaxed-volunteer test data and those for the braced-volunteer test data, the total controller for posture and force has the potential to decrease forward displacement but to increase downward displacement. This indicates that the force controller had a significant effect on head excursions in the anteroposterior direction.

Expression of the Braced Condition

To simulate the braced condition, Meijer et al. [4] set higher co-contraction levels of antagonist muscles than in the relaxed condition. They simultaneously contracted both agonist and antagonist muscles, thus co-contracting muscles around joints without producing any net moment. However, even in maintaining occupant postures, real humans in the braced condition can increase muscular forces and generate forces at the steering wheel and the pedals. Figure 6 shows that the newly developed total control of posture and force generated forces at the steering wheel and pedals, although the force at the steering wheel was smaller than that from test data. The reason for the difference in steering forces between the simulation results with total control of posture and force and the volunteer test data is probably the modeling of the wrist or muscle activation in the trunk or shoulder. Further studies are needed for sufficient constraints on rotations of the wrist and forearm and for determination of reasonable percentage contributions of muscles in the shoulder or trunk.

In this study, the newly developed muscle controller calculated muscle activations by summation of muscle activations predicted by the posture control and those predicted by the force control, as shown in Equation (5). The posture control generated muscle forces to keep joint angles from changing while the force control generated muscle forces to push the hands or feet against the steering wheel or pedals, respectively. Although the force control tended to work against the posture control, total control of posture and force has the potential to increase forces and to reproduce forces similar to those obtained from the test data without changing the posture.

CONCLUSIONS

In this study, a muscle activation controller including two feedback controls of posture and

force using PID control was newly developed to predict occupant kinematics in braced conditions during low-speed impacts. The controller was used to predict muscle activation with THUMS version 5 including whole-body muscle models, and was validated against the observed kinematics of cadavers or volunteers during low-speed frontal impacts with 5.0 G and 2.5 G decelerations. The simulation results for head excursions without muscle activation, with posture control, and with total control of posture and force generally agreed with those from cadaver test data, relaxed volunteer test data, and braced volunteer test data, respectively. In addition, the forces predicted at the pedals showed good agreement with those from the test data in the braced condition, although the forces predicted at the steering wheel were smaller than those in the test data. Although further studies of optimization methods are needed in order to determine valid PID gain parameters for various dynamic environments, the developed controller showed the potential for more accurate prediction of both relaxed- and braced-occupant kinematics closer to those of real occupants than when using the previous controller.

ACKNOWLEDGEMENTS

The authors would like to thank Drs. Tsuyoshi Yasuki and Yuichi Kitagawa and Mr. Shigeki Hayashi and Mr. Hiroshi Miyazaki for their constant support in our research. The authors also would like to thank the Toyota Research Institute of North America (TRI-NA) and Virginia Tech for conducting collaborative research in the low-speed frontal impact sled tests using volunteers and cadavers.

REFERENCES

[1] Ejima, S., Zama, Y., Satou, F., Holcombe, S., Ono, K., Kaneoka, K., and I. Shiina. 2008. “Prediction of the physical motion of the human body based on muscle activity during pre-impact braking.” Proceedings of the IRCOBI Conference; Bern, Switzerland.

[2] Beeman, S.M., Kemper, A.R., Madigan, M.L., Duma, S.M. 2011. “Effects of bracing on human kinematics in low-speed frontal sled tests.” Annals of Biomedical Engineering 39, No. 12, 2998–3010.

[3] Beeman, S.M., Kemper, A.R., Madigan, M.L., Franck, C.T., and S.C. Loftus. 2012. “Occupant kinematics in low-speed frontal sled tests: Human volunteers, Hybrid III ATD, and PMHS.” Accident analysis and prevention 47, 128–139.

[4] Meijer, R., Broos, J., Elrofai, H., de Bruijn, E., Forbes, P., and R. Happee. 2013. “Modelling of bracing in a multi-body active human model.” Proceedings of the IRCOBI Conference; Gothenburg, Sweden.

[5] Östh, J., Brolin, K., and D. Bråse. 2015. “A human body model with active muscles for simulation of pretensioned restraints in autonomous braking interventions.” Traffic Injury Prevention 16, 304–313.

[6] Iwamoto, M., Nakahira, Y., Tamura, A., Kimpara, H., Watanabe, I., and K. Miki. 2007. “Development of advanced human models in THUMS.” Proceedings of the 6th European LS-DYNA Users’ Conference; Gothenburg, Sweden.

[7] Östh, J., Eliasson, E., Happee, R., and K. Brolin. 2014. “A method to model anticipatory postural control in driver braking events.” Gait and Posture 40, No. 4, 664–669.

[8] Hault-Dubrulle, A., Robache, F., Drazétic, P., and H. Morvan. 2009. “Pre-crash phase analysis using a driving simulator. Influence of atypical position on injuries and airbag adaptation.” Proceedings of the 21st ESV Conference; Stuttgart, Germany. Paper No. 09-0534.

[9] Iwamoto, M., Nakahira, Y., and H. Kimpara. 2015. “Development and validation of the Total HUman Model for Safety (THUMS) toward further understanding of occupant injury mechanisms in precrash and during crash.” Traffic Injury Prevention 16, Suppl. 1, S36–S48.

[10] Iwamoto, M., and Y. Nakahira. 2015. “Development and validation of the Total HUman Model for Safety (THUMS) version 5 containing multiple 1D muscles for estimating occupant motions with muscle activation during side impacts.” Stapp Car Crash Journal 59, 53–90.

[11] Kato, D., Kimpara, H., Nakahira, Y., and M. Iwamoto. 2016. “Effects of controlled muscle activations on human head–neck responses during low-speed rear impacts.” Proceedings of the IRCOBI Asia Conference; Seoul, South Korea.

[12] Géradin, M. and A. Cardona. 2001. “Flexible Multibody Dynamics: A Finite Element Approach.” John Wiley & Sons Ltd., West Sussex, England.

[13] Agur, A.M.R. and A.F. Dalley. 2005. “Grant's Atlas of Anatomy,” Eleventh Edition. Lippincott Williams & Wilkins, Baltimore, MD, USA.

[14] Iwamoto, M., Nakahira, Y., Kimpara, H., Sugiyama, T., and K. Min. 2012. “Development of a human body finite element model with multiple muscles and their controller for estimating occupant motions and impact responses in frontal crash situations.” Stapp Car Crash Journal 56, 231–268.

[15] Gehre, C., Gades, H., and Wernicke, P. 2009. “Objective rating of signals using test and simulation responses.” Proceedings of the 21st ESV Conference; Stuttgart, Germany. Paper No. 09-0407.

[16] Gehre, C., and Stahlschmidt, S. 2011. “Assessment of dummy models by using objective rating methods.” Proceedings of the 22nd ESV Conference; Washington, DC, USA. Paper No. 11-0216.

[17] van Rooij, L. 2011. “Effect of various pre-crash braking strategies on simulated human kinematic response with varying levels of driver attention.” Proceedings of the 22nd ESV Conference; Washington, D.C., USA. Paper No. 11–0306.

[18] Cappon, H., Mordaka, J., van Rooij, L., Adamec, J., Praxl, N., and H. Muggenthaler. 2007. “A Computational Human Model with Stabilizing Spine: A Step Towards Active Safety.” SAE International, Warrendale, PA, USA. SAE Technical Paper No. 2007–01–1171.

APPENDICES

Estimation Method for Reaction Forces

The current version of LS-DYNA R8.0.0 cannot perform feedback control for reaction forces even though it can perform feedback control for displacements. Therefore, we inserted four small elastic boxes between the feet and the pedals and between the hands and the steering wheel to estimate the reaction forces from the box deformations, and performed feedback for the estimated forces. The boxes, which were shaped as rectangular parallelepipeds, were modeled using a linear isotropic elastic material. The rotations of the contact surfaces between the boxes and the human body were constrained at the surfaces of the steering and pedals. Generally, the axial force F (N) was calculated based on the axial deformation Δl (mm) in the direction perpendicular to the contact surface as follows:

$$F = \frac{E \cdot A}{l} \cdot \Delta l \qquad \textbf{(Equation A1)}$$

where E (N/mm^2) is the Young's modulus of the box, A (mm2) is the cross-sectional area of the contact surface, and l (mm) is the original length in the direction perpendicular to the contact surface. Additionally, by setting Poisson's ratio to 0, the shear force Q (N) was calculated based on the shear deformation Δx (mm) as follows:

$$Q = \frac{E \cdot A}{2l} \cdot \Delta x . \qquad \textbf{(Equation A2)}$$

This is because of the isotropic elastic material property of the box. The reaction force of each part was estimated as a resultant force. To validate this estimation method, we performed a simulation in which the right pedal was pushed with the linear isotropic elastic box. Figure A1 shows the comparison of simulation results between reaction forces estimated from deformation and post-processed contact force between the right foot and the right pedal. The simulation results indicate that the calculation method has acceptable accuracy.

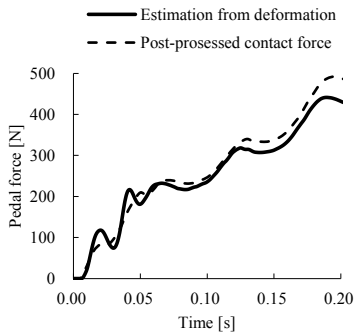

Figure A1. Comparison of estimated force and predicted contact force for a pedal force.

Table A1.
Percentage contributions of some muscles on right lower extremity (add: adduction, abd: abduction, e: extension, f: flexion, ir: internal rotation, er: external rotation).

Percentage contribution	*R*				*P*
		Hip joint		Knee joint	Right pedal force
Muscle name	+: add -: abd	+: e -: f	+: ir -: er	+: f -: e	
Psoas Major	0.00	-1.00	0.00	0.00	0.00
Iliacus	0.00	-1.00	0.00	0.00	0.00
Sartorius	-0.10	-0.30	-0.30	0.30	0.00
Rectus Femoris	0.00	-0.50	0.00	-0.50	0.00
Tensor Fasciae Latae	-0.35	-0.35	0.30	0.00	0.00
Piriformis	-0.25	0.25	-0.50	0.00	0.00
Superior Gemellus	0.00	0.20	-0.80	0.00	0.00
Inferior Gemellus	0.00	0.20	-0.80	0.00	0.00
Obturator Externus	0.50	0.00	-0.50	0.00	0.00
Obturator Internus	0.00	0.20	-0.80	0.00	0.00
Quadratus Femoris	0.50	0.00	-0.50	0.00	0.00
Gluteus Minimus	-0.80	0.00	0.20	0.00	0.00
Gluteus Medius	-0.80	0.00	0.20	0.00	0.00
Gluteus Maximus	0.00	0.70	-0.30	0.00	0.30
Semitendinosus	0.00	0.40	0.20	0.40	0.00
Semimembranosus	0.00	0.40	0.20	0.40	0.00
Biceps Femoris Long Head	0.00	0.50	0.00	0.50	0.10
Biceps Femoris Short Head	0.00	0.00	0.00	1.00	0.00
Adductor Brevis	0.80	-0.20	0.00	0.00	0.00
Adductor Longus	0.80	-0.20	0.00	0.00	0.00
Adductor Magnus	0.90	0.10	0.00	0.00	0.00
Pectineus	0.90	-0.10	0.00	0.00	0.00
Gracilis	0.30	-0.30	0.20	0.20	0.00
Vastus Lateralis	0.00	0.00	0.00	-1.00	0.30
Vastus Intermedius	0.00	0.00	0.00	-1.00	0.30
Vastus Medialis	0.00	0.00	0.00	-1.00	0.30
Popliteus	0.00	0.00	0.00	1.00	0.00